

A full network coupled to the evolutionary code: detailed s -process nucleosynthesis in low mass AGB Stars

S. Cristallo¹, O. Straniero¹, R. Gallino²

¹ Osservatorio Astronomico di Collurania, via Mentore Maggini, 64100 Teramo, Italy; e-mail: cristallo@te.astro.it, straniero@te.astro.it

² Dipartimento di Fisica Generale, Università di Torino e Sezione INFN di Torino, via P. Giuria 1, 10125 Torino, Italy

Abstract. In the FRANEC code, a full set of equations describing the physical evolution of a star is coupled with the nuclear processes fixing the temporal variation of the nuclear species. Mixing induced by convection is calculated by means of a time dependent algorithm, where the efficiency of the process is taken proportional to the convective velocity. In the computation of AGB stellar models, we assume an exponentially decaying profile of the velocity at the inner border of the convective envelope, which allows the formation of a tiny ^{13}C -pocket after a third dredge up episode. The s -process nucleosynthesis occurring in an AGB star of initial mass $M=2 M_{\odot}$ and solar metallicity is presented.

Key words. AGB stars – nucleosynthesis – s -process

1. The network

The model presented here has been obtained by adopting a network including about 500 isotopes (ranging from neutron up to the Pb-Bi-Po ending point) involving more than 750 reactions. We updated the network in its completeness and then we focused our attention not only on neutron captures and beta decays (the two processes strictly interacting during the s -process), but also on reactions involving the capture of charged particles (protons and α). A detailed description of the reaction network is reported in the following five subsections: n-

capture reactions (1.1), n production reactions (1.2), charged particles capture reactions (1.3), β decay reactions (1.4) and treatment of isomeric states (1.5).

1.1. n -captures reactions

By n -capture reactions we mean (n,γ) , (n,α) and (n,p) processes. For the (n,γ) reactions, we used as a reference compilation the cross sections tabulated in Bao et al. (2000, hereafter BK2000). In that paper, experimental and theoretical data are listed as a function of the thermal energy from 5 to 100 keV. We then integrated the uncovered energy ranges with cross sections taken from the database obtained with the NON-SMOKER code (Rauscher &

Send offprint requests to: S. Cristallo

Correspondence to: Osservatorio Astronomico di Collurania, via M. Maggini, 64100 Teramo

Thielemann 2000, hereafter RT2000), and we merged data renormalizing the theoretical value at 30 keV to the BK2000 one (this is our standard procedure for all processes inserted in the network with the exception of weak interactions). Concerning the cross sections not listed in BK2000, we directly used data provided by RT2000 over the whole temperature range. In the last four years many isotope cross sections have been remeasured or theoretically revisited by several authors, so we upgraded the network with the most recent results available in the literature. With regard to Si isotopes we refer to Guber et al. (2003), Cl isotopes to Guber et al. (2002), ^{60}Ni to Corvi et al. (2002), ^{62}Ni to Rauscher et al. (2002), ^{88}Sr to Koehler et al. (2000), Kr isotopes to Gallino et al. (2002), Xe isotopes to Reifarth et al. (2002), Cd isotopes to Wisshak et al. (2002), ^{139}La to O'Brien et al. (2003), Pm isotopes to Reifarth et al. (2003), ^{151}Sm and Eu isotopes to Best et al. (2001) and finally Pt isotopes to Koehler et al. (2002a). The (n, α) and (n,p) cross reactions involving heavy isotopes are taken from RT2000, while for the lighter ones we adopted data from different authors. We choose the $^{14}\text{N}(n,p)^{14}\text{C}$ from Koehler et al. (1989), the $^{17}\text{O}(n,\alpha)^{14}\text{C}$ from Wagemans et al. (2002), the $^{26}\text{Al}(n,p)^{26}\text{Mg}$ from Koehler et al. (1997), the $^{26}\text{Al}(n,\alpha)^{23}\text{Na}$ from Wagemans et al. (2001) and the $^{33}\text{S}(n,\alpha)^{30}\text{Si}$ from Schatz et al. (1995). The $^{35}\text{Cl}(n,p)^{35}\text{S}$ rate is taken from Druyts et al. (1994), the $^{36}\text{Cl}(n,p)^{36}\text{S}$ and the $^{36}\text{Cl}(n,\alpha)^{33}\text{P}$ from Wagemans et al. (2003), the $^{37}\text{Ar}(n,p)^{37}\text{Cl}$ and the $^{37}\text{Ar}(n,\alpha)^{34}\text{S}$ from Goeminne et al. (2001), the $^{39}\text{Ar}(n,\alpha)^{36}\text{S}$ from Goeminne (2001) and finally the $^{41}\text{Ca}(n,p)^{41}\text{K}$ and the $^{41}\text{Ca}(n,\alpha)^{38}\text{Ar}$ from Wagemans et al. (1998).

1.2. Neutron production reactions

During the AGB phase, the main neutron sources are the $^{13}\text{C}(\alpha,n)^{16}\text{O}$ and the $^{22}\text{Ne}(\alpha,n)^{25}\text{Mg}$ (see Gallino et al. 1998). The $^{13}\text{C}(\alpha,n)^{16}\text{O}$ reaction has never been measured at typical astrophysical energies (8 keV) and the extrapolation of experimental points to this range of temperatures remains problematic, due to the presence of a subthreshold reso-

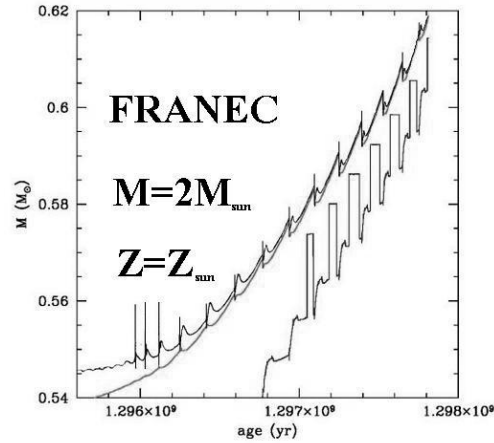


Fig. 1. Thermal pulse AGB phase for a star with initial mass $M=2 M_{\odot}$ and solar metallicity. See main text for details.

nance. Our choice focused over the work of Drotleff et al. (1993). However the use of a different rate (Kubono et al. 2002, Angulo et al. 1998) doesn't involve a consistent alteration of the final surface isotopic distribution, as demonstrated by Cristallo et al. (2004) and Pignatari et al. (2004). The study of the $^{22}\text{Ne}(\alpha,n)^{25}\text{Mg}$ is more complicated, owing to the presence of subthreshold resonances (Koehler et al. 2002b). We adopted the lower limit of Kaeppeler et al. (1994), ignoring the resonance at 633 keV. The 828 keV resonance was given a strength equal to its 1σ lower limit, that is $164 \mu\text{eV}$.

1.3. Charged particle capture reactions

Reaction rates of isotopes involving charged particles are taken from the NACRE compilation (Angulo et al. 1998), while, if the reaction is not present in this database, we used values from Caughlan & Fowler (1988, hereafter CF88) and other authors (Rauscher & Thielemann 2000, Formicola et al. 2004, Caughlan et al. 1985, Thielemann et al. 1987, Kunz et al. 2002). With regard to the $^{14}\text{N}(p,\gamma)^{15}\text{O}$, we used recent values obtained by the LUNA experiment (see Formicola et al. 2004). Being the bottleneck of the CNO burn-

ing, this reaction has an enormous importance in stellar evolution. The new low energy values are about a factor 2 lower than previous data by Schroeder et al. (1987) which were adopted by CF88 and NACRE.

1.4. β decay reactions

Weak interaction rates (electron captures, β and positron decays) are interpolated as a function of the temperature (from 10^7 K to 10^{10} K) and electron density (from 1 to 30 cm^{-3}). At temperatures lower than 10^7 K we assume a constant value equal to the terrestrial one. For isotopes up to ^{37}Ar , data have been taken from Oda et al. (1994), with the exception of ^7Be (Caughlan & Fowler 1988) and the isomeric state of ^{26}Al , for which we refer to Coc et al. (2000). With regard to unstable isotopes between ^{39}Ar and ^{45}Ca we use prescriptions by Fuller et al. (1982), while between ^{45}Ca and ^{64}Cu (excluding ^{63}Ni) we follow Langanke & Martínez-Pinedo (2000). For ^{63}Ni and heavier isotopes we use the rates tabulated in Takayashi & Yokoi (1987), with the exceptions of ^{79}Se and ^{176}Lu , for which we refer respectively to Klay & Kaeppler (1988) and Klay et al. (1991). For the few rates not included in any compilation, we directly use the terrestrial value in the whole range of energies.

1.5. Isomeric states

In a stellar plasma, the presence of the isomeric states can lead to the ramification of the s -process flux into two different components and then it can give rise to important branching points. The cases of importance we have treated concern branching points originated by the isomeric state of ^{26}Al , ^{85}Kr , ^{176}Lu and ^{180}Ta . With regard to production of ^{26}Al , we splitted the proton capture on ^{25}Mg in to two distinct reactions: the first to create $^{26}\text{Al}^g$ (*i.e.* its ground state, characterized by a $\tau \simeq 740$ Ky in terrestrial conditions; we refer to paragraph 1.4 for the treatment of this decay in the stellar interiors) and the second to create $^{26}\text{Al}^m$ (the isomeric state of ^{26}Al – we assume it decays instantaneously to ^{26}Mg). Concerning ^{85}Kr , ^{84}Kr

can produce, on capturing a free neutron, $^{85}\text{Kr}^m$ with a probability of about 50% with respect to the total (n,γ) cross section. $^{85}\text{Kr}^m$ has a non-zero probability to decay by internal conversion to its ground state (about 20%), thus leading to the following branching ratio:

$$R = \frac{\sigma(^{84}\text{Kr}(n,\gamma)^{85}\text{Kr}^m)}{\sigma(^{84}\text{Kr}(n,\gamma)^{85}\text{Kr}^{tot})} = 0.42. \quad (1)$$

With regard to the branching at $^{176}\text{Lu}^g$, we assumed the isomeric state to decay instantaneously to ^{176}Hf , while the ground state, which in terrestrial condition is practically stable, to have an half-life depending on the temperature (see section 1.4). For an estimation of the population-ratio of the two possible states, we refer to Klay et al. (1991) who suggest:

$$B = \frac{\sigma(^{175}\text{Lu}(n,\gamma)^{176}\text{Lu}^g)}{\sigma(^{175}\text{Lu}(n,\gamma)^{176}\text{Lu}^{tot})} = 0.11 \quad (2)$$

Between $E=20$ keV and $E=40$ keV we assumed $B=0.5$. An improved treatment of this branching is needed, after more precise cross sections of Lu and Hf isotopes become available (F. Kaeppler, *private communication*). Finally, for the treatment of the branching between the isomeric and ground states of ^{180}Ta , we refer to Nemeth et al. (1992), where the isomeric ratio is given as a function of the temperature.

2. The model

Results presented here refer to a star with initial mass $M=2 M_{\odot}$ and solar metallic calculated by means of the version of the FRANEC stellar evolutionary code described by Chieffi et al. (2001); a period- dM/dt relation, as obtained by fitting observational data reported by Whitelock et al. (2003), is combined with a period-luminosity relation for AGB stars (Groenewegen et al. 2003) to compute the mass loss rate of the model. Figure 1 describes the TP-AGB phase, which starts when $M_{\text{H}} \simeq 0.55 M_{\odot}$. The three lines illustrate the evolution of the positions, in mass coordinates, of (top to bottom): the inner border of the convective envelope, the maximum energy production

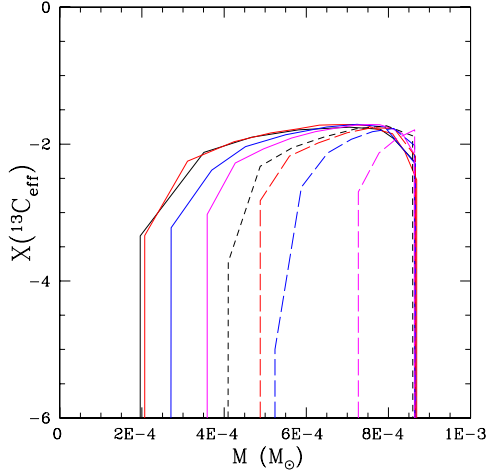


Fig. 2. Evolution of the ^{13}C -pocket after subsequent TDUs.

within the H-burning shell and the maximum energy production within the He-intershell.

After a couple of thermal pulses without third dredge-up (TDU), a series of eight thermal pulses followed by TDU takes place. Note that the first TDU episode occurs earlier than previously found in our computations (Straniero et al. 1997). This is a consequence of the inclusion of the exponential decline of the convective velocity at the convective boundary. The velocity usually drops to zero at the neutral point, where the adiabatic temperature gradient is equal to the radiative temperature gradient. In this situation our new algorithm does not produce any significant difference with respect to the previous computation. However, when the convective instability penetrates the H depleted region, $\nabla_{rad} \gg \nabla_{ad}$ at the most internal mesh points of the convective envelope and the convective velocity substantially grows above zero. In other words, the (formal) border of the convective envelope does not coincide with the neutral point. In this condition, the assumed exponential decline of the convective velocity induces a partial mixing of H in the region located immediately below the formal boundary of convection that rapidly becomes fully unstable. In such a way a deeper penetration of the convec-

tive envelope naturally develops. In Table 1 we report the total mass, the core mass, the mass of the dredged up material and the surface C/O ratio obtained pulse by pulse: the strength of the TDU reaches a maximum and, then, drops as a consequence of the envelope reduction caused by the mass loss. The C/O ratio in the envelope grows up to a final value of 1.67 at the last TP with TDU. The model attains the C-star stage when the core mass is just $0.57 M_{\odot}$.

Table 1. Total mass, core mass, dredged up material and C/O ratio for thermal pulses with TDU.

Pulse n.	M_{tot} (M_{\odot})	M_H (M_{\odot})	M_{dup} ($10^{-3} M_{\odot}$)	C/O
1	1.901	0.561	0.4	0.33
2	1.894	0.568	1.5	0.36
3	1.878	0.575	2.5	0.46
4	1.843	0.583	3.5	0.61
5	1.771	0.590	4.4	0.82
6	1.650	0.596	4.2	1.06
7	1.457	0.603	4.7	1.36
8	1.196	0.609	3.5	1.67
9	0.923	0.615	0.07	1.67

During the interpulse phase, a ^{13}C -pocket forms where, after the TDU, the receding convective envelope leaves an increasing profile of protons. The extension in mass of the ^{13}C -pocket decreases pulse after pulse. In Figure 2 the effective $X(^{13}\text{C}_{eff}) = X(^{13}\text{C}) - X(^{14}\text{N})$ characterizing each ^{13}C -pocket is plotted (this quantity is representative of the real dimension of the pocket, because of the strong poisoning effect of the $^{14}\text{N}(n,p)^{14}\text{C}$ reaction): starting from a mass extension of about $10^{-3} M_{\odot}$ at the first pulse with TDU, the pocket shrinks down to $10^{-4} M_{\odot}$ at the last pulse with TDU. When the temperature of the ^{13}C -pocket becomes as large as 9×10^7 K, the $^{13}\text{C}(\alpha, n)^{16}\text{O}$ reaction and s-process nucleosynthesis take place. The first two pockets are only marginally consumed before the onset of the following thermal pulse, while, subsequently, the ^{13}C is fully burned in the radiative interpulse phase (see Straniero et al. 1995). The $^{22}\text{Ne}(\alpha, n)^{25}\text{Mg}$ reaction is very

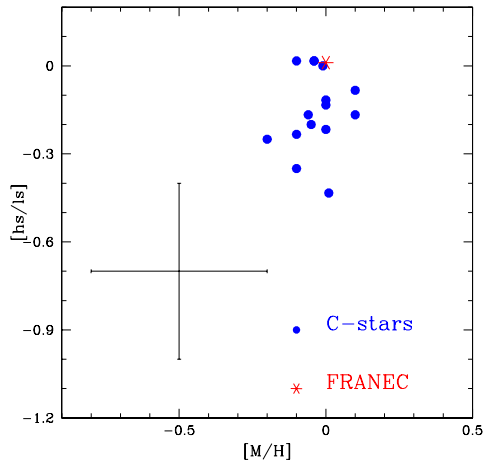


Fig. 3. Observed [hs/ls] ratio of a sample of Galactic CN stars, compared with our theoretical prediction.

marginally activated at the base of the convective region generated by a thermal pulse.

3. Conclusion

As a preliminary test, we have compared our theoretical results with the observed composition of Galactic CN stars, as reported by Abia et al. (2002). We extracted from that sample stars with a clear detection of ^{99}Tc and compared it with our theoretical prediction, when the surface ratio $\text{C}/\text{O} \approx 1$. The estimated ratio between the hs (Ba, La, Nd) and the ls (Y, Zr) appears in good agreement with those derived from the spectroscopic analysis (see Figure 3).

Acknowledgements. Work partly supported by the Italian MURST-FIRB project “The Astrophysical Origin of the Heavy Elements beyond Iron”. S.C. thanks the ‘7th Torino Workshop’ organizers at the Institute of Astronomy, Cambridge for the coverage of the local expenses and for the useful and interesting discussions carried on during this meeting.

References

Abia C., et al., 2002, *ApJ*, 579, 817
 Angulo C., et al. 1999, *Nucl. Phys. A*, 656, 3
 Bao Z. Y., et al., 2000, *Atom. Data Nucl. Data Tables*, 76, 70

Best J., et al., 2001, *Phys. Rev. C*, 64, 015801
 Caughlan G. R., et al., 1985, *Atom. Data Nucl. Data Tables*, 32, 197
 Caughlan G. R., Fowler W. D., 1988, *Atom. Data Nucl. Data Tables*, 40, 283
 Chieffi A., et al., 2001, *ApJ*, 554, 1159
 Coc A., et al., 2000, *Phys. Rev. C*, 61, 015801
 Corvi F., et al., 2002, *Nucl. Phys. A*, 697, 581
 Cristallo S., et al., 2004, in the Proceedings of *Nuclei in the Cosmos VIII*, *Nucl. Phys. A*, submitted
 Drotleff H. W., et al., 1993, *ApJ*, 414, 735
 Druyts S., et al., 1994, *Nucl. Phys. A*, 573, 291
 Formicola A., et al., 2004, *Phys. Lett. B*, 591, 61
 Fuller G.M., et al., 1982, *ApJS*, 48, 279
 Gallino R., et al., 1998, *ApJ*, 497, 388
 Gallino R. et al., 2002, in the Proceedings of the *11th Workshop on Nuclear Astrophysics*, MPA, Garching, 205
 Goeminne G., et al., 2001, *Nucl. Phys. A*, 688, 233
 Goeminne G., 2001, PhD Thesis
 Groenewegen M.A.T., et al., 1996, *MNRAS*, 281, 1347
 Guber K. H., et al., 2002, *Phys. Rev. C*, 65, 058801
 Guber K. H. et al., 2003, *Phys. Rev. C*, 67, 062802
 Kaeppeler F., et al., 1994, *ApJ*, 437, 396
 Klay N., Kaeppeler F., 1988, *Phys. Rev. C*, 38, 295
 Klay N., et al., 1991, *Phys. Rev. C*, 44, 2839
 Koehler P. E., O’Brien H. A., 1989, *Phys. Rev. C*, 39, 1655
 Koehler P. E., et al., 1997, *Phys. Rev. C*, 56, 1138
 Koehler P. E., et al., 2000, *Phys. Rev. C*, 62, 055803
 Koehler P. E., et al., 2002a, *J. Nucl. Sci. and Technology Suppl.*, 2, 546
 Koehler P. E., et al., 2002b, *Phys. Review C*, 66, 055805
 Kubono S., et al., 2003, *Phys. Rev. Lett.*, 90, 062501
 Kunz R., et al., 2002, *ApJ*, 567, 643
 Langanke K., Martínez-Pinedo G., 2000, *Nucl. Phys. A*, 673, 481
 Nemeth Zs., et al., 1992, *ApJ*, 392, 277

- O'Brien S., et al., 2003, Phys. Rev. C, 68, 035801
- Oda T., et al., 1994, Atom. Data Nucl. Data Tables, 56, 231
- Pignatari M., et al., 2004, in the Proceedings of Nuclei in the Cosmos VIII, Nucl. Phys. A, *submitted*
- Rauscher T., Thielemann F. K., 2000, Atom. Data Nucl. Data Tables, 75, 1
- Rauscher T., Guber K. H., 2002, Phys. Rev. C, 66, 028802
- Reifarth R., et al., 2002, Phys. Rev. C, 66, 064603
- Reifarth R., et al., 2003, ApJ, 582, 1251
- Schatz H., et al., 1995, Phys. Rev. C, 51, 379
- Schroeder U., et al., 1987, Nucl. Phys. A, 467, 240S
- Straniero O., et al., 1995, ApJ, 440L, 85S
- Straniero O., et al., 1997, ApJ, 478, 332S
- Takahashi K., Yokoi K., 1987, Atom. Data Nucl. Data Tables, 36, 375
- Thielemann F., et al., 1987, Adv. Nucl. Astrophys., 525
- Wagemans C., et al., 1998, Phys. Rev. C, 57, 1766
- Wagemans J., et al., 2001, Nucl. Phys. A, 696, 31
- Wagemans J., et al., 2002, Phys. Rev. C, 65, 034614
- Wagemans C., et al., 2003, Nucl. Phys. A, 719, 127
- Whitelock P.A., et al., 2003, MNRAS, 342, 86
- Wisshak K., et al., 2002, Phys. Rev. C, 66, 025801